Effects of Pb substitution on the vortex state of oxygen-overdoped $Bi_2Sr_2CaCu_2O_{8+\delta}$ single crystal

D. Darminto
Department of Physics, Bandung Institute of Technology, Jl. Ganesa 10, Bandung 40132, Indonesia and Department of Physics, Faculty of Mathematics and Science, Sepuluh Nopember Institute of Technology, Sukolilo, Surabaya 60111, Indonesia

M. O. Tjia
Department of Physics, Bandung Institute of Technology, Jl. Ganesa 10, Bandung 40132, Indonesia

T. Motohashi, H. Kobayashi, Y. Nakayama, J. Shimoyama, and K. Kishio
Department of Superconductivity, The University of Tokyo, 7-3-1 Hongo, Bunkyo-ku, Tokyo 113-8656, Japan
(Received 22 February 2000; revised manuscript received 10 May 2000)

We show that excessive Pb substitution of Bi in oxygen-overdoped BSCCO-2212 single crystal further reduces the anisotropy (ρ_c/ρ_a ratio) of the system in addition to enhancing disorder in its vortex system. These effects have led to the suppression of first-order vortex melting as well as a peculiar second-peak effect exhibiting a sensitive temperature dependence over an unusually broad temperature range. Our experimental data further reveal, in a Bi-based system, the presence of a disentangled vortex liquid phase separating the solid vortex from the entangled vortex liquid phase in the *H-T* diagram constructed from the transport and magnetization data.

INTRODUCTION

The unusually rich variety of vortex phases in the *H-T* phase diagram is one of the most remarkable features distinguishing the new copper oxide superconductors from the conventional type-II superconductors. The appearance of a vortex liquid phase over a large area in the *H-T* diagram initiated intensive research on the structure and characteristics of the liquid phase as well as the true nature of the related thermodynamical transition across its boundary with the solid phase. It has now been established theoretically[1–5] and confirmed experimentally[6–12] that vortex melting in a clean sample is a first-order transition, while the presence of disorder is likely to change its character into a more gradual or second-order process.

It is also well known that the traditional picture of the solid vortex phase has been greatly modified by the presence of disorder and anisotropy. It has been found necessary to include, in addition to the ordered vortex lattice state at low *H* and *T*, the less ordered or disordered glassy state at the higher *H-T* regime. This is further complicated by the occurrence of dimensional crossover at a certain boundary within the solid phase.[2,8,13–15] Studies on second-peak effects in BSCCO-2212 superconductors also suggest further complications of the solid vortex phase.[16,17]

No less complicated is the vortex liquid phase where a multiphase structure emerges as a result of the intricate interplay among the thermal fluctuation effect, the pinning, and Lorentz forces as well as the plastic response of the vortex lines in highly anisotropic superconductors. The BSCCO-2212 superconductor, among others, offers a particularly rich and novel phenomenology of the vortex system due to its high T_c and strongly layered structure. It has thus become one of the most intensely studied systems to date. It is theoretically predicted that apart from the metal-like viscous liquid phase of entangled vortices,[18,19] an additional intermediate phase of disentangled vortices may exist as the pinned vortex liquid.[20] This picture is further enriched by the presence of a decoupled two-dimensional (2D) ''pancake'' vortex phase at the high-*H* and -*T* regime. The entangled (E) and disentangled (DE) phases are supposed to exhibit different transport characteristics, and can hence be investigated from measurements of their transport properties. While the possible existence of the more elusive disentangled phase has been discussed in previous reports on YBCO-123,[21–23] BSCCO-2212,[12] and an artificial layered MoGe/Ge system,[24] a more concrete experimental picture have so far been reported in YBCO-124 only.[25] Obviously, additional studies are required before a more comprehensive picture of this particular vortex phase emerges.

As mentioned above, anisotropy and disorder of the high-T_c superconductor play crucial roles in affecting the characteristics of the vortex solid and vortex liquid phases as well as the vortex-melting behavior in high-T_c superconductors. It is well known that excessive oxygen doping generally introduces disorder into the crystal structure[26] and reduces its degree of anisotropy as well.[15,27,28] Partial substitution of Bi by Pb in the system is expected to have additional effects of the same kind.[29,30] In order to study the vortex characteristics due to those effects, we have prepared nonleaded and leaded BSCCO-2212 single crystals which are overdoped with oxygen. The results of the characterizations and vortex phase analysis of our samples will be presented on the basis of transport data for the vortex liquid phase and the magnetization data for the vortex solid phase.

EXPERIMENT

The single-crystalline samples of $Bi_{2.1}Sr_{1.8}CaCu_2O_x$ and $Bi_{1.6}Pb_{0.6}Sr_{1.8}CaCu_2O_y$ were grown from the corresponding

feed rods by means of the floating zone technique in an image furnace of NEC SC-M15HD equipped with double ellipsoidal mirrors. The growing process for the leaded sample was performed with a relatively higher growth rate of 0.5 mm/h to suppress the sublimation loss of Pb. Details of the process are described in Ref. 29. To produce the oxygen-overdoped (OV) samples, cleaved single crystals obtained from a cut of the grown boules were annealed at 400 °C for 72 h in oxygen with a partial pressure of 2.1 atm in a sealed quartz tube. This post-annealing treatment resulted in $T_{c,on} \sim 77.6$ K and 65 K in a zero external field for the nonleaded and leaded samples, respectively.

The in-plane resistive transition curves (ρ_a, ρ_b) were measured by the standard dc four-probe method, whereas the out-of-plane resistivity (ρ_c) measurements were similarly carried out with current electrodes consisting of annular rings as further described in Ref. 30. These resistivity measurements were conducted by using a fixed current of 10 mA in an external magnetic field applied along the *c* axis and varied from 100 Oe to 10 kOe. The magnetization measurement was carried out by means of a Quantum Design superconducting quantum interference device (SQUID) magnetometer (MPMS XL-5s) in the magnetic field which was also applied along the *c* axis up to 15 kOe, with temperature variation in the range of 10–55 K.

RESULTS AND DISCUSSION

The data presented in Figs. 1(a) and 1(b) are the resistive transition curves measured along the *a* and *b* axes, respectively, from the leaded sample, while Fig. 1(c) is the result obtained from the nonleaded sample. We have found it important to compare the $\rho_a(T)$ and $\rho_b(T)$ curves from the leaded sample, since Pb-doped BSCCO-2212 single crystals have been reported to exhibit modulated structure along the *b* axis at doping levels below a certain value.[29,31] This anisotropic in-plane structure is supposed to give rise to different transport behaviors along the two different axes. The close resemblance between $\rho_a(T)$ and $\rho_b(T)$ displayed in the figures indicates that the sample is relatively free from such a modulation effect, which may well be due to the relatively rich Pb content in our sample as suggested in Refs. 29 and 31.

We further observe from those figures that none of the resistivity curves in the whole range of the magnetic field feature the typical sharp drop associated with first-order vortex melting such as those commonly found in the YBCO-123 (Refs. 6, 7, 32 and 33) and nonleaded BSCCO-2212 samples,[12,34–36] including those overdoped with oxygen.[37] For comparison, we have also presented in Fig. 1(c) the $\rho_{ab}(T)$ curves of our nonleaded sample. The sharp melting feature is clearly visible for $H \leqslant 1$ kOe, in agreement with result reported previously.[37] Apparently, the additional presence of Pb has introduced additional disorder such that vortex melting as seen in Figs. 1(a) and 1(b) has become a more gradual process instead of a sharp first-order transition observed in cleaner samples. In this case it is more appropriate to speak of the irreversible temperature T_{irr} determined by the ''finite-resistivity criterion'' $\rho(T_{irr})/\rho_n = 10^{-4}$, which marks the border between the dissipative and nondissipative temperature regimes.

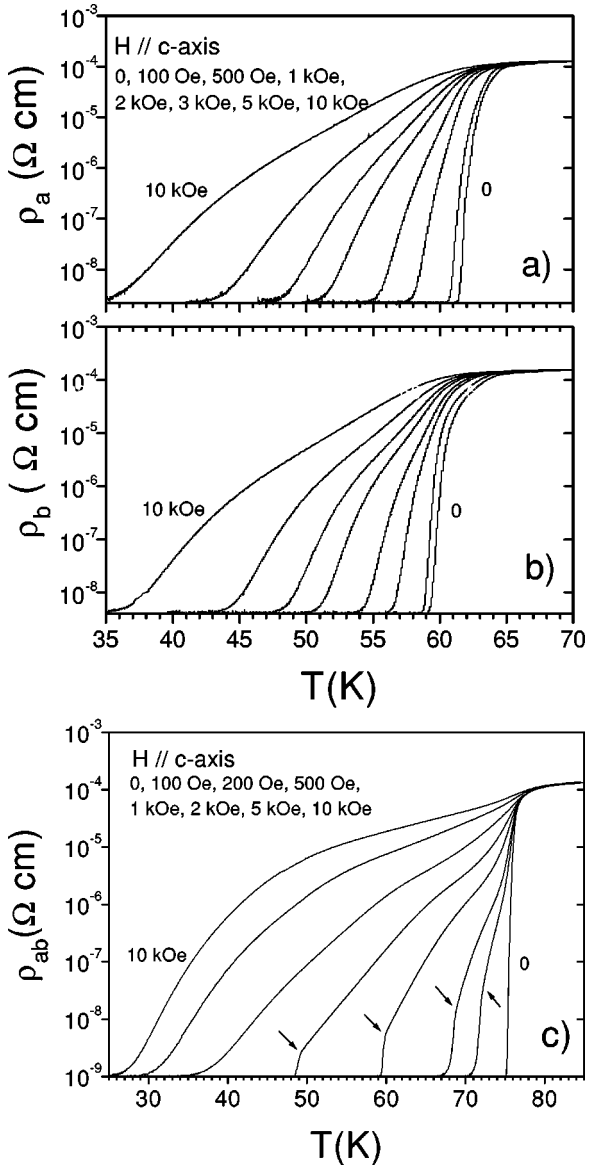

FIG. 1. In-plane resistive transition curves measured on leaded sample along the (a) *a* axis, $\rho_a(T)$, (b) *b* axis, $\rho_b(T)$, and that measured on nonleaded sample (c) $\rho_{ab}(T)$. All measurements were performed in external magnetic field applied parallel *c* axis and ranging from 0 to 10 kOe. The arrowheads in (c) indicate sharp melting transitions.

It is interesting to note, on the other hand, that shoulder structures indicated by changes of slope are clearly visible on both $\rho_a(T)$ and $\rho_b(T)$ in Figs. 1(a) and 1(b), respectively, in particular at higher magnetic fields. This commonly shared feature of the two sets of transport data, in conformity with their generally close resemblance mentioned earlier, is thus supposed to be intrinsic in nature. This shoulder structure has been theoretically predicted as an indication of crossover between a pinned vortex liquid and unpinned vortex liquid, which would otherwise show up as a sharp kink for a disorder-free sample.[7,20] A similar feature has been reported in YBCO-123 (Refs. 7 and 22) and BSCCO-2212.[38] These two liquid regimes were either assigned as the TAFF and FF regimes[20] or two distinct (low and high) TAFF regimes.[22,25] One may further explore a possible correlation between these two regimes with the disentangled and entangled vortex

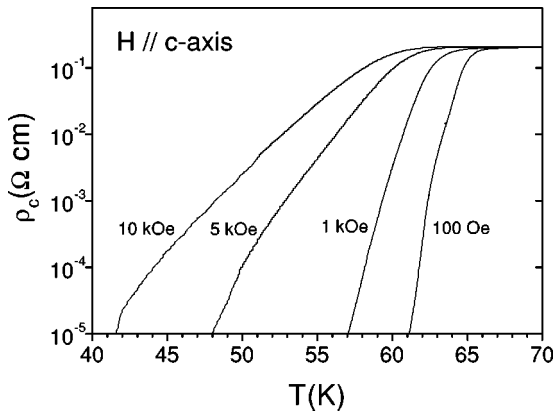

FIG. 2. Longitudinal resistive transition curves $\rho_c(T)$ measured on the leaded sample in an external magnetic field applied along the c axis with various strengths.

phases, respectively. This possibility will be examined later in connection with the out-of-plane transport data $\rho_c(T)$.

The result of the $\rho_c(T)$ measurement in the same range of magnetic field is given in Fig. 2. In view of the close resemblance between $\rho_a(T)$ and $\rho_b(T)$, we have determined the resistivity ratio $\gamma^2=\rho_c/\rho_a$ from data in Fig. 1(a) and Fig. 2. The resulting curves at various fields are shown in Fig. 3. It is seen that γ^2 varies considerably with the external magnetic field and depends sharply on temperature around the T_c which is supposed to decrease at higher external field. We recall that the temperature-dependent behavior of γ has been predicted theoretically for layered superconductors based on a simple model of pancake-diffusion-induced phase slip between neighboring pancake layers.[39] According to this model, the general trend can be described by the formula

$$\frac{\rho_{ab}}{\rho_c}=C\frac{\Phi_0^2 s^2 E_J^2}{BT^2}. \tag{1}$$

In this expression, $C=\pi/[\ln(nr_{max}^2)\ln(r_{max}/a_0)]$ where r_{max} is the upper cutoff of the phase coherence distance, a_0 = average intervortex spacing, s = interlayer spacing, and E_J is the Josephson coupling energy given by $E_J=\Phi_0^2/(4\lambda\gamma)^2\pi^3 s$, where γ is the Ginzburg-Landau anisotropy ratio. It was shown that the data obtained from Bi-2212

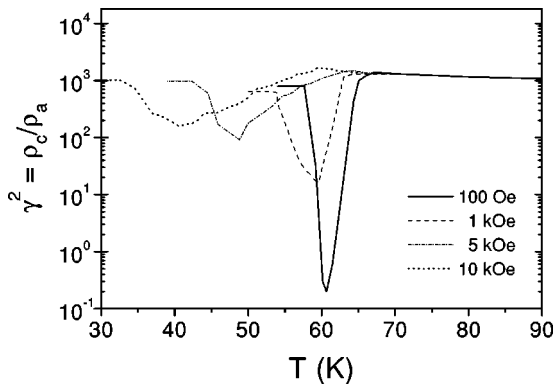

FIG. 3. Temperature dependence of the resistivity ratio measured on the leaded sample at various external magnetic fields applied parallel c axis.

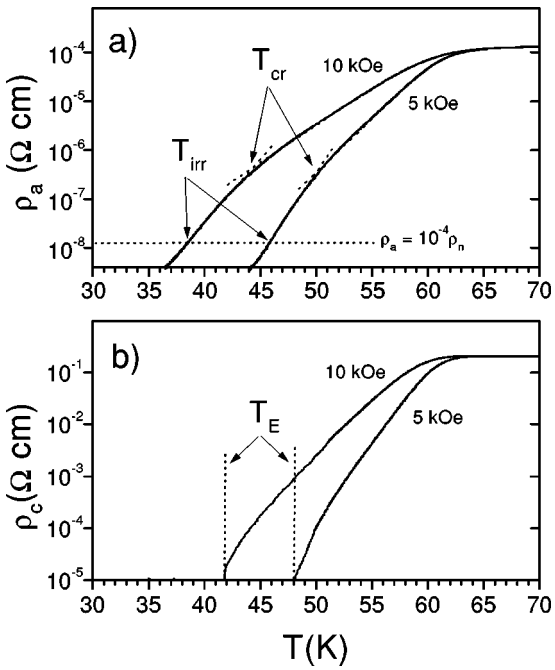

FIG. 4. (a) Close-up view of $\rho_a(T)$ at high fields taken from Fig. 1(a), displaying shoulder structures and the associated crossover temperatures T_{cr}. (b) $\rho_c(T)$ curves corresponding to the same magnetic fields taken from Fig. 2 indicating T_E associated with $\rho_c(T_E)=0$. See text for explanation on the correlation between the two figures.

sample[40] in the temperature range of 45–70 K for an external field varied between 0.5 and 2 T could be satisfactorily fitted by using the relation $E_J\alpha\ (1-T/T_c)^2$ and replacing the B^{-1} dependence in Eq. (1) by $B^{-0.52}$. Apart from the qualitatively similar temperature- and field-dependent behaviors shown by our data, the numerical value of ρ_c/ρ_a (hereforth denoted by γ^2) determined in this experiment deviates significantly from Eq. (1). It shows instead a much narrower range of T dependence at low fields, resembling a dip near the associated T_c. This dip appears broadened and shifted in accordance with the lowering of the corresponding T_c, and perceptibly suppressed as the external field increases, in qualitative agreement with the BSCCO data considered in Ref. 39. We note, however, that this experimental result yields the value $\gamma^2=650$–1010 at temperatures away from the corresponding T_c's, with the minimum around T_c given by $\gamma^2<1$ for $H=100$ Oe and $\gamma^2=160$ for $H=10$ kOe. These values are generally an order of magnitude smaller than the range of γ^2 cited for clean BSCCO crystal.[12,15] Using the values $\gamma^2=650$–1010, we are led to the 2D decoupling field of $H_{2D}=8.6$–13.4 kOe, according to the standard formula $H_{2D}=\Phi_0/(\gamma s)^2$.

In order to address the issue of the possible correlation between the shoulder structure and the presence of a pinned vortex liquid, we show in Figs. 4(a) and 4(b), respectively, the close-up views of two high-field $\rho_a(T)$ curves, each from Fig. 1(a), and two high-field $\rho_c(T)$ curves from Fig. 2. As described in Fig. 4(a), the crossover temperature (T_{cr}) is determined as the point where a change of slope occurs on $\rho_a(T)$. It is remarkable to observe the near coincidences at both fields between T_{cr} and T_E, the temperature where $\rho_c=0$ which marks the disappearance of dissipation for longi-

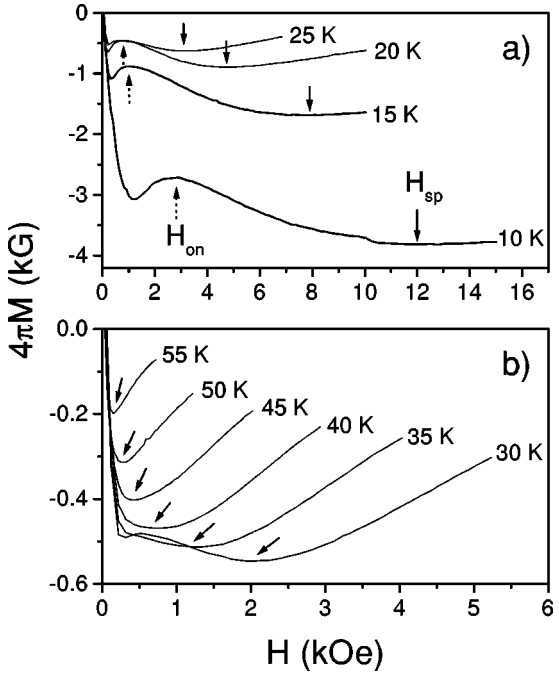

FIG. 5. Magnetization curves of the leaded BSCCO-2212 single crystal measured in the temperature range (a) 10–25 K and (b) 30–55 K. The arrowheads indicate the second-peak fields on those curves.

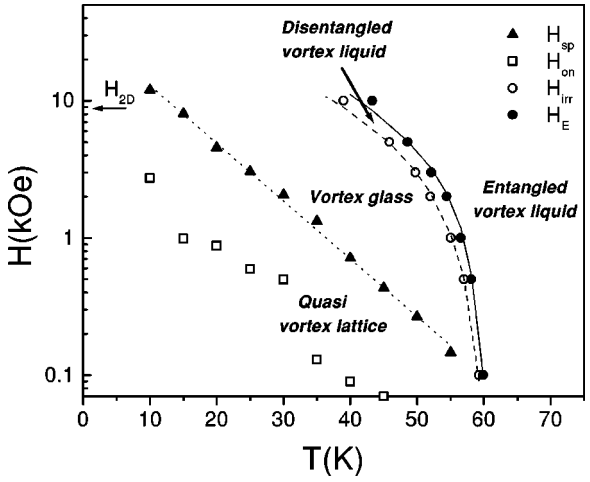

FIG. 6. Vortex phase diagram of oxygen-overdoped $Bi_{1.6}Pb_{0.6}Sr_{1.8}CaCu_2O_y$ single crystal, derived from transport and magnetization data as explained in the text. The dotted, dashed, and solid lines are results of the best fits with theoretical models discussed in the text.

tudinal current flow. This occurrence of $\rho_c=0$ at T_E can be attributed to diminishing vortex line movement, in conjunction with the crossover from the entangled vortex liquid at higher T to the disentangled or pinned vortex liquid at lower T as predicted theoretically on the basis of 2D vortex boson model.[41] It was argued that the condition expressed by $H_m(T)<H<[1/(3c_L)]^4H_m(T)$ which is well satisfied in this case[20] signifies the existence of a new, truly thermodynamic phase of pinned vortex liquid with a large plastic deformation time scale. In a disordered sample such as the one considered here, the transition between the entangled and disentangled phases revealed by $\rho_c(T_E)=0$ will be more appropriately described as a more gentle crossover process as manifested by the weak shoulder structure in $\rho_a(T)$. Due to the relatively weak shoulder structure, the coincidence between T_E and T_{cr} over the entire field range shown in Figs. 1(a), 1(b), and 2 appears less than perfect. Nevertheless, the consistent closeness between their values should constitute a serious indication for the correlation we set out to show.

The magnetization data of the leaded sample measured at various temperatures are presented in Figs. 5(a) and 5(b). It is observed that the second peaks are generally much broader than those observed in the nonleaded samples prepared in this experiment as well as results on a similar sample reported in previous works.[42] We also note that the peak effect in the leaded sample persists in a much larger temperature range than those exhibited by the nonleaded samples mentioned above. It is further shown by the figures that the peak field H_{sp} defined by the minimum in a magnetization curve as denoted in the figures exhibits remarkable temperature-dependent behavior, rising rapidly with decreasing temperature, in clear contrast to the more or less temperature-independent feature exhibited by our nonleaded samples, confirming an earlier report on a similar sample. These temperature-dependent behaviors of H_{sp} have in fact been reported also on NCCO (Refs. 43 and 44) and TBCO.[45] It is understood that the peak effect is generally associated with the transition between the ordered vortex quasilattice and the disordered (entangled) vortex glass states. The onset of this effect at H_{on} is also understood to signify enhanced effectiveness of pinning due to higher flexibility of the vortex line lattice at higher temperature. This effect disappears at H_{sp} in conjunction with the destruction of 3D order due to a higher magnetic field and higher temperature. In general, Pb substitution and overdoping by oxygen are known to reduce anisotropy while introducing disorder in the meantime. The second peak is therefore expected to better survive the thermal fluctuation effect, and may well persist up to the vicinity of T_c due to stronger vortex coupling and more effective pinning.[46] It is also reasonable to expect that H_{sp} tends to decrease as T approaches T_c and merges eventually with the vortex melting line (or irreversible line in this case). In the same vein, the low-temperature part of H_{sp} is found to appear at a higher field compared to that observed on the nonleaded sample in connection with the lower γ and hence higher crossover field H_{2D}. We shall further pursue the significance of this point in more detail in the ensuing discussions.

To this end, we shall concentrate on the data of the leaded sample. These data are summarized in a H-T phase diagram as depicted by Fig. 6. We note first of all that a plot of the peak effect onset field H_{on} has been added to the figure, based on previously measured data[47] for $T>30$ K and our current data for $T\leqslant 30$ K [Fig. 5(a)]. It must be stressed that the values of H_{on} for $T>30$ K cannot be determined from our measurement due to heavy overlaps among the magnetization curves in that temperature range as seen in Fig. 5(b). The H_{sp} curve was readily obtained as a plot of the corresponding data points indicated in those two figures. The border between the solid and liquid phases is represented by an irreversible line (IL) determined from the values of T_{irr} for each H in Fig. 4. Finally, the crossover line between the disentangled and entangled liquid phases is obtained by plot-

ting the data points (T_E and H_E) for $\rho_c=0$ in the same figure.

Before proceeding further with our discussion, let us recall the expression derived by Nelson[19] on the basis of the 2D boson model for the crossover line between the entangled and disentangled vortex liquid phases as given by

$$H_E(T)=H_0\left(\frac{1}{T}-\frac{1}{T_c}\right), \tag{2}$$

where $H_0=\gamma\xi_{ab}(0)[\Phi_0 H_{c2}(0)]^{3/2}/(4L\mu_0\kappa^2\pi^{3/2})$ and L is the sample thickness. This model predicts that the disentangled phase in the H-T phase diagram shrinks as L increases and vanishes eventually as $L\rightarrow\infty$. Our data can be nicely fitted with Eq. (2) for $T_c=63.5$ K and $H_0=1282.1$ kOe K in the field range $H<10$ kOe, namely, more or less below our estimated 2D decoupling field H_{2D}. However, if we adopt the value $\xi_{ab}(0)=3.02$ nm, $H_{c2}(0)=360$ kOe, and $\kappa=89.3$ given by our magnetization data and $\gamma^2=1000$ from our transport data, we end up with a value of L much too small compared to its real value as already pointed out in a previous report.[22] It should be recalled in this connection that similar formulas having the same T dependence have been derived by Daemen *et al.*[48] and Ikeda[49] on different grounds, with different expressions for H_0 where the interlayer distance s appears explicitly in place of L. We have found that using Ikeda's formula ($H_0=\Phi_0^3/[4\pi^2\mu_0 k_B s\gamma^2\lambda_{ab}^2(0)]$), and the values $s=1.54$ nm, $\lambda_{ab}(0)=270$ nm, our H_0 yields the result $\gamma^2=857$, which is well within the range observed in this experiment. We hasten to stress though that this should not be taken as an indication favoring a 3D-2D decoupling transition instead of a DE-E transition, since the region considered here lies below H_{2D}, and the appearance of nonvanishing ρ_c as we cross the H_E line to the right does not necessary imply the complete decoupling of the pancake vortices into a 2D system. It is perhaps useful at this point to refer to the work of Gray *et al.*,[50] who pointed out that the presence of some pancake vortex correlation may persist even above the thermal decoupling temperature, and further effects of the vortex-vortex interaction should be taken into account in all those models before a proper analysis and interpretation of the data could be made.

We note further that the data for irreversible or melting points are consistently located to the left of the $H_E(T)$ line. The best fit of these data with the more or less standard functional form[3,51] $H_{irr}(T)=H_{irr}(0)(1-T/T_c)^m$ is achieved for $H_{irr}(0)=44.06$ kOe and $m=1.53$, which is supposed to indicate the dominance of the combined effect of thermal and quantum fluctuations.[51,52] One observes from Fig. 5 that there is some indication of deviation from this behavior at lower temperature and higher field, similar to those reported in BSCCO,[53,54] TBCO,[45] and NCCO.[44,54] A thorough study of this phenomenon is still needed to reveal its detailed underlying physical mechanism. It is tempting at this point to consider the empirical formula proposed by Kitazawa *et al.*,[55] namely,

$$H_{irr}(T)=\frac{33400}{\gamma^2}\left(1-\frac{T}{T_c}\right)^m. \tag{3}$$

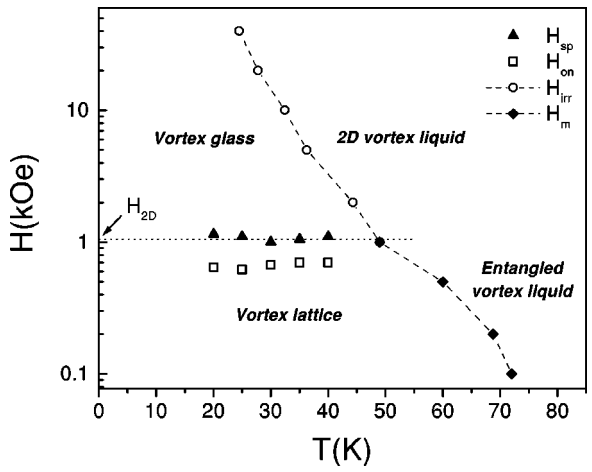

FIG. 7. Vortex phase diagram of oxygen-overdoped $Bi_{2.1}Sr_{1.8}CaCu_2O_x$ single crystal. The dotted and dashed lines are guides to the eyes. The explanation is given in the text.

Equating the multiplicative factor in this equation with the value of $H_{irr}(0)$ obtained above yields the result $\gamma^2=758$, which is still in the same ballpark as the value mentioned earlier.

Moving to the lower-temperature regime in the diagram, we find a vortex glass phase bounded from the left by the second-peak field line $H_{sp}(T)$. As seen from the figure, the associated data fit extremely well with the exponential relation[45] given by $H_{sp}(T)=H_{s0}\exp(-T/T_0)$ for $H_{s0}=34.17$ kOe and $T_0=10.3$ K. This curve clearly displays a highly sensitive temperature-dependent behavior. Additionally, the second peak appears to persist in the entire temperature range below T_c. In particular, a rough estimate of the 3D-2D crossover field $H_{2D}=\Phi_0/(\gamma s)^2$ using the value $\gamma^2=857$ leads to a value of H_{sp} ($T=10$ K) which is located within the range of H_{2D} determined in this experiment. We note, however, that apart from displaying a general trend of decline with increasing temperature, the $H_{on}(T)$ data appear to undergo a discernable change of slope around $T=35$ K. Apparently only piece-wise fitting is possible for $H_{on}(T)$, and a coherent description is lacking from the existing models. This should become a subject of further study.

Having gone through the lengthly discussions about the new features in the vortex phases of the leaded sample, a comparation with the H-T diagram of our nonleaded oxygen-overdoped sample will be in order. For this purpose, the H-T diagram constructed from our data on this sample is presented in Fig. 7. It is clear that the diagram shares the same features with other results reported previously,[17,47] which also pointed out the resemblance of these features with those of the optimally doped Bi-2212 crystals. We note first of all that no disentangled phase appears in the diagram, as the entangled vortex liquid phase is directly bounded from its solid phase by the melting line. As mentioned earlier, another remarkable departure from the phase diagram shown in Fig. 6 is the practically flat H_{sp} line with its low-temperature end located at the 2D decoupling field H_{2D} of about 1 kOe which is considerably lower than that in the leaded case. The second-peak field of this nonleaded sample is terminated at its low-temperature part by the zero-dimensional pinning limit at about 20 K, while the high-temperature part of H_{sp} is

smoothly joined by its melting line $H_m(T)$. In other words, the flat H_{sp} curve in the limited temperature region appears as the border line between the 3D and 2D vortex solids. This is in marked contrast to the highly sensitive T dependence of H_{sp} in the leaded case, which divides the solid vortex phase into the quasivortex lattice and glass phases in the 3D vortex region over nearly the entire temperature range below T_c instead of merging with the melting line. Further, the second-peak region in the H-T diagram is much more confined in Fig. 7 than that in Fig. 6. These remarkably different features consistently support the view of the enhanced effectiveness of pinning due to Pb substitution as alluded earlier. This in turn is ascribable to the delicate combined effect, of increased disorder and anisotropy suppression. Nevertheless, a thorough understanding of their underlying mechanism as well as those discrepancies found in the leaded sample between our data and the existing models warrants further and more detailed studies on the subject.

CONCLUSION

We have shown in this work that excessive substitution of Bi by Pb in oxygen-overdoped BSCCO-2212 single crystal has affected significant changes on the transport and magnetic properties of the system. The disorder effect introduced in this case results in the suppression of the first-order vortex melting process commonly observed in nonleaded samples. Meanwhile, the combined effect of higher disorder and lower anisotropy has produced broadened second peaks over an usually broad temperature range with highly sensitive temperature-dependent behavior hitherto unknown in nonleaded samples. Most remarkable of all, our experimental data have revealed the existence of a disentangled vortex liquid in the H-T phase diagram of the Bi-based system, presumably due to the combined effect alluded to above. Meanwhile, our data have also shown some discrepancies with existing theoretical models and hence the need of further studies on the experimental as well as theoretical aspects of this subject.

ACKNOWLEDGMENTS

One of us (D.D.) would like to thank The Matsumae International Foundation for supporting his research at The University of Tokyo. This work was also partially supported by a RUT research grant under Contract No. 207/SP/RUT/BPPT/IV/97 of Indonesia and NEDO and CREST/JST of Japan.

[1] M.P.A. Fisher, Phys. Rev. Lett. **62**, 1415 (1989).
[2] M.V. Feigel'man, V.B. Geshkenbein, and A.I. Larkin, Physica C **167**, 177 (1990).
[3] A. Houghton, R. Pelcovits, and A. Sudbo, Phys. Rev. B **40**, 6763 (1989).
[4] D.R. Nelson and V.M. Vinokur, Phys. Rev. Lett. **68**, 2398 (1992).
[5] A.I. Larkin and V.M. Vinokur, Phys. Rev. Lett. **75**, 4666 (1995).
[6] H. Safar, P.L. Gammel, D.A. Huse, D.J. Bishop, J.P. Rice, and M. Ginsberg, Phys. Rev. Lett. **69**, 824 (1992).
[7] W.K. Kwok, S. Fleshler, U. Welp, V.M. Vinokur, J. Downey, G.W. Crabtree, and M.M. Miller, Phys. Rev. Lett. **69**, 3370 (1992); W.K. Kwok, J.A. Fendrich, U. Welp, S. Fleshler, J. Downey, and G.W. Crabtree, *ibid.* **72**, 1088 (1994); W.K. Kwok, J.A. Fendrich, S. Fleshler, U. Welp, J. Downey, and G.W. Crabtree, *ibid.* **72**, 1092 (1994).
[8] R. Cubitt, E.M. Forgan, G. Yang, S.L. Lee, D.Mc.K. Paul, H.A. Mook, M. Yethiraj, P.H. Kes, T.W. Li, A.A. Menovsky, Z. Tarnawski, and K. Mortensen, Nature (London) **365**, 407 (1993).
[9] E. Zeldov, D. Majer, M. Konczykowski, V.B. Geshkenbein, V.M. Vinokur, and H. Shtrikman, Nature (London) **375**, 373 (1995).
[10] S.L. Lee, M. Warden, H. Keller, J.W. Schneider, D. Zech, P. Ziemermann, R. Cubitt, E.M. Forgan, M.T. Wylie, P.H. Kes, T.W. Li, A.A. Menovsky, and Z. Tarnawski, Phys. Rev. Lett. **75**, 922 (1995).
[11] A. Schilling, R.A. Fisher, N.E. Phillips, U. Welp, D. Dasgupta, W.K. Kwok, and G.W. Crabtree, Nature (London) **382**, 791 (1996).
[12] D.T. Fuchs, E. Zeldov, D. Majer, R.A. Doyle, T. Tamegai, S. Ooi, and M. Konczykowski, Phys. Rev. B **54**, R796 (1996); D.T. Fuchs, R.A. Doyle, E. Zeldov, D. Majer, W.S. Seow, R.J. Drost, T. Tamegai, S. Ooi, M. Konczykowski, and P.H. Kes, *ibid.* **55**, R6156 (1997).
[13] G. Yang, P. Shang, S.D. Sutton, I.P. Jones, J.S. Abell, and C.E. Gough, Phys. Rev. B **48**, 4054 (1993).
[14] T. Tamegai, I. Oguro, Y. Iye, and K. Kishio, Physica C **213**, 33 (1993).
[15] K. Kishio, J. Shimoyama, Y. Kotaka, and K. Yamafuji, in *Proceeding of the Seventh International Workshop on Critical Currents in Superconductors*, edited by H. Weber (World Scientific, Singapore, 1994), p. 339.
[16] E. Zeldov, D. Majer, M. Konczykowski, A.I. Larkin, V.M. Vinokur, V.B. Geshkenbein, N. Chikumoto, and H. Shtrikman, Europhys. Lett. **30**, 367 (1995).
[17] B. Khaykovich, E. Zeldov, D. Majer, T.W. Li, P.H. Kes, and M. Konczykowski, Phys. Rev. Lett. **76**, 2555 (1996).
[18] D.R. Nelson, and H.S. Seung, Phys. Rev. B **39**, 9153 (1989).
[19] D. R. Nelson, in *Phenomenology and Applications of High Temperature Superconductors*, edited by K. Bedell *et al.* (Addison-Wesley, New York, 1991).
[20] G. Blatter, M.V. Feigel'man, V.B. Geshkenbein, A.I. Larkin, and V.M. Vinokur, Rev. Mod. Phys. **66**, 1125 (1994).
[21] D. Lopez, E.F. Righi, G. Nieva, and F. de la Cruz, Phys. Rev. Lett. **76**, 4034 (1996).
[22] X.G. Qiu, B. Wuyts, M. Maenhoudt, V.V. Moshchalkov, and Y. Bruynseraeda, Phys. Rev. B **52**, 559 (1995).
[23] A.V. Samoilov, M.V. Feigel'man, M. Konczykowski, and H. Holtzberg, Phys. Rev. Lett. **76**, 2798 (1996).
[24] D.G. Steel, W.R. White, and J.M. Graybeal, Phys. Rev. Lett. **71**, 161 (1993).
[25] X.G. Qiu, V.V. Moshchalkov, Y. Bruynseraeda, and J. Karpinski, Phys. Rev. B **58**, 8826 (1998).
[26] L. Miu, G. Jakob, P. Haibach, F. Hillmer, H. Adrian, and C.C. Almasan, Phys. Rev. B **57**, 3151 (1998).
[27] Y. Kotaka, T. Kimura, H. Ikuta, J. Shimoyama, K. Kitazawa, K. Yamafuji, K. Kishio, and D. Pooke, Physica C **235-240**, 1529 (1994).

[28] C. Bernhard, C. Wenger, Ch. Niedermayer, D.M. Pooke, J.L. Tallon, Y. Kotaka, J. Shimoyama, K. Kishio, D.R. Noakes, C.E. Stronach, T. Sembiring, and E.J. Ansaldo, Phys. Rev. B **52**, R7050 (1995).

[29] I. Chong, Z. Hiroi, M. Izumi, J. Shimoyama, Y. Nakayama, K. Kishio, T. Terashima, Y. Bando, and M. Takano, Science **276**, 770 (1997).

[30] T. Motohashi, Y. Nakayama, T. Fujita, K. Kitazawa, J. Shimoyama, and K. Kishio, Phys. Rev. B **59**, 14 080 (1999).

[31] Z. Hiroi, I. Chong, and M. Takano, J. Solid State Chem. **138**, 98 (1998).

[32] M. Charalambous, J. Chaussy, P. Lajay, and V.M. Vinokur, Phys. Rev. Lett. **71**, 436 (1993).

[33] W. Jiang, N.C. Yeh, D.S. Reed, U. Kriplani, and F. Holtzberg, Phys. Rev. Lett. **74**, 1438 (1995).

[34] S. Watauchi, H. Ikuta, J. Shimoyama, and K. Kishio, Physica C **259**, 373 (1996).

[35] K. Kadowaki, Physica C **263**, 164 (1996).

[36] C.D. Keener, M.L. Trawick, S.M. Ammirata, S.E. Hebboul, and J.C. Garland, Phys. Rev. B **55**, R708 (1997).

[37] H. Ikuta, S. Watauchi, H. Kobayashi, Y. Nakayama, J. Shimoyama, K. Kitazawa, and K. Kishio, Physica C **282-287**, 2015 (1997).

[38] D.T. Fuchs, R.A. Doyle, E. Zeldov, S.F.W.R. Rycroft, T. Tamegai, S. Ooi, M.L. Rappaport, and Y. Myasoedov, Phys. Rev. Lett. **81**, 3944 (1998).

[39] A.E. Koshelev, Phys. Rev. Lett. **76**, 1340 (1996).

[40] R. Bush, G. Ries, H. Werthner, G. Kreiselmeyer, and G. Saemann-Ischenko, Phys. Rev. Lett. **69**, 522 (1992).

[41] M.V. Feigel'man, V.B. Geshkenbein, and V.M. Vinokur, Pis'ma Zh. Eksp. Teor. Fiz. **52**, 1141 (1990) [JETP Lett. **52**, 546 (1990)].

[42] J. Shimoyama, Y. Nakayama, K. Kitazawa, K. Kishio, Z. Hiroi, I. Chong, and M. Takano, Physica C **281**, 69 (1997).

[43] D. Giller, A. Shaulov, R. Prosorov, Y. Abulafia, Y. Wolfus, L. Burlachkov, Y. Yesurun, E. Zeldov, V.M. Vinokur, J.L. Peng, and R.L. Greene, Phys. Rev. Lett. **79**, 2542 (1997).

[44] A.A. Nugroho, I.M. Sutjahja, M.O. Tjia, A.A. Menovsky, F.R. de Boer, and J.J.M. Franse, Phys. Rev. B **60**, 15 379 (1999).

[45] F. Zuo, S. Khizroev, G.C. Alexandrakis, and V.N. Kopylov, Phys. Rev. B **52**, R755 (1995).

[46] V.M. Vinokur, B. Khaykovich, E. Zeldov, M. Konczykowski, R.A. Doyle, and P.H. Kes, Physica C **295**, 209 (1998).

[47] J. Shimoyama, Y. Nakayama, T. Motohashi, T. Fujita, T. Yamada, K. Sugita, K. Kitazawa, K. Kishio, Z. Hiroi, I. Chong, and M. Takano, in *Proceedings of the 10th International Symposium on Superconductivity (ISS'97)*, edited by K. Osamura and I. Hirabayashi (Springer-Verlag, Tokyo, 1998), p. 279.

[48] L.L. Daemen, L.N. Bulaevskii, M.P. Maley, and J.Y. Coulter, Phys. Rev. Lett. **70**, 1167 (1993).

[49] R. Ikeda, J. Phys. Soc. Jpn. **64**, 1683 (1995).

[50] K.E. Gray, J.D. Hettinger, D.J. Miller, B.R. Eashburn, C. Moreau, C. Lee, B.G. Glagola, and M.M. Eddy, Phys. Rev. B **54**, 3622 (1996); K.E. Gray, D.G. Steel, J.D. Hettinger, D.J. Miller, B.R. Washburn, M. Ware, J.T. Parkman, M.E. Yoder, C. Moreau, and M.M. Eddy, IEEE Trans. Appl. Supercond. **7**, 1987 (1997).

[51] C.C. Almasan, M.C. de Andrade, Y. Dalichaouch, J.J. Neumeier, C.L. Seaman, M.B. Maple, R.G. Guertin, M.V. Kurie, and J.C. Garland, Phys. Rev. Lett. **69**, 3812 (1992).

[52] G. Blatter and B. Ivlev, Phys. Rev. Lett. **70**, 2621 (1993).

[53] A. Schilling, J. Jin, J.D. Guo, and H.R. Ott, Phys. Rev. Lett. **71**, 1899 (1993).

[54] M.C. de Andrade, N.R. Diley, F. Ruess, and M.B. Maple, Phys. Rev. B **57**, R708 (1998).

[55] K. Kitazawa, J. Shimoyama, H. Ikuta, T. Sasagawa, and K. Kishio, Physica C **282-287**, 335 (1997).